Correlation among Order−Disorder, Electronic Levels, and Photoluminescence in Amorphous CT:Sm

Alberthmeiry T. de Figueiredo,*,† Sergio de Lazaro,† Elson Longo,‡ Elaine C. Paris,† José A. Varela,‡ Miryam R. Joya,§ and Paulo S. Pizani§

LIEC/CMDMC, Departamento de Química, UFSCar, Via Washington, Km 235, CP-676, CEP-13565-905, São Carlos, SP, Brazil, Instituto de Química, Universidade Estadual Paulista, CEP 14800-900, Araraquara, SP, Brazil, and Departamento de Física, Universidade Federal de São Carlos, Caixa Postal 676, São Carlos, 13565-905 SP, Brazil

Received February 16, 2006

$Ca_{0.95}Sm_{0.05}TiO_3$ (CT:Sm) powder was prepared by the polymeric precursor method (PPM). Order−disorder at short and long range has been investigated by means of Raman spectroscopy, X-ray diffraction (XRD), and photoluminescence emission (PL) experimental techniques. The broad PL band and the Sm emission spectrum measured at room temperature indicate the increase of structural order with annealing temperature. The measured PL emission reveals that the PL intensity changes with the degree of disorder in the CT:Sm. The electronic structures were performed by the ab initio periodic method in the DFT level with the hybrid nonlocal B3LYP approximation. Theoretical results are analyzed in terms of DOS, charge densities, and Mulliken charges. Localized levels into the band gap of the CT:Sm material favor the creation of the electron−hole pair, supporting the observed room-temperature PL phenomenon.

Introduction

It is well-known that production of new photoluminescent materials is very attractive for modern technology. The $ATiO_3$ (A = Pb, Ca, Sr, and Ba) perovskites have attracted considerable attention and constitute one of the most important classes of mixed oxides, suitable for various applications due to their physical properties, and have been extensively studied as candidates for electrooptical devices.[1,2] Much interest has been dedicated to the study of photoluminescence (PL) in nanostructured[3−6] or amorphous[7−9] materials since the first time visible PL at room temperature was observed in porous silicon.[10] Rare-earth ions are used to dope perovskite-type oxides not only as a probe to investigate local centers and energy[11−14] but also to provoke changes in the optical behavior[15] or improve the capacitance response making it possible to use these ceramics as high-frequency ultrasonic transducers.[16] Our research group has demonstrated that amorphous titanates displayed intense visible PL at room temperature.[17,18]

The PL phenomenon at room temperature occurs due to structural disorder of the system. Therefore, if the system is totally disordered, the PL does not exist; as well, a system totally ordered does not exhibit PL.[19] In such cases, a minimal order in the system is necessary for the material to exhibit PL. X-ray absorption near edge structure (XANES) results on the $SrTiO_3$ amorphous phase[20] pointed out the coexistence of two types of environments for the titanium, namely, a five-fold (TiO_5) square-base pyramid and a six-fold coordination (TiO_6) octahedron. Order is related to the presence of TiO_6 clusters, whereas the disorder is related to the presence of TiO_5 clusters. PL emission occurs due to

* To whom correspondence should be addressed. E-mail: alberth@liec.ufscar.br or sergio@liec.ufscar.br

† UFSCar.

‡ Universidade Estadual Paulista.

§ Universidade Federal de São Carlos.

(1) Lee, S. Y.; Custodio, M. C. C.; Lim, H. J.; Feigelson, R. S.; Maria, J. P.; Trolier-McKinstry, S. *J. Cryst. Growth* **2001**, *226*, 247.
(2) Muralt, P. *J. Micromech. Microeng.* **2000**, *10*, 136.
(3) Xiong, H. M.; Liu, D. P.; Xia, Y. Y.; Chen, J. S. *Chem. Mater*. **2005**, *17*, 3062.
(4) Fujihara, S.; Ogawa, Y.; Kasai, A. *Chem. Mater*. **2004**, *16*, 2965.
(5) Draeger, E. W.; Grossman, J. C.; Williamson, A. J.; Galli, G. *J. Chem. Phys*. **2004**, *120*, 10807.
(6) Farmer, S. C.; Patten, T. E. *Chem. Mater*. **2001**, *13*, 3920.
(7) Orhan, E.; Pontes, F. M.; Pinheiro, C. D.; Boschi, T. M.; Leite, E. R.; Pizani, P. S.; Beltran, A.; Andres, J.; Varela, J. A.; Longo, E. *J. Solid State Chem*. **2004**, *177*, 3879.
(8) Bol, A. A.; van Beek, R.; Meijerink, A. *Chem. Mater*. **2002**, *14*, 1121.
(9) Westin, G.; Ekstrand, A.; Zangellini, E.; Borjesson, L. *J. Phys. Chem. Solids* **2000**, *61*, 67.
(10) Canham, L. T. *Appl. Phys. Lett*. **1990**, *57*, 1046.
(11) Kyomen, T.; Sakamoto, R.; Sakamoto, N.; Kunugi, S.; Itoh, M. *Chem. Mater*. **2005**, *17*, 3200.
(12) Dunbar, T. D.; Warren, W. L.; Tuttle, B. A.; Randall, C. A.; Tsur, Y. *J. Phys. Chem. B* **2004**, *108*, 908.
(13) Aitasalo, T.; Deren, P.; Holsa, J.; Jungner, H.; Krupa, J. C.; Lastusaari, M.; Legendziewicz, J.; Niittykoski, J.; Strek, W. *J. Solid State Chem*. **2003**, *171*, 114.
(14) Diallo, P. T.; Jeanlouis, K.; Boutinaud, P.; Mahiou, R.; Cousseins, J. C. *J. Alloys Compd*. **2001**, *323*, 218.
(15) Block, B. A.; Wessels, W. *Appl. Phys. Lett*. **1994**, *65*, 25.
(16) Li, K.; Pang, G.; Wa Chan, H. L.; Choy, C. L.; Li, J. H. *J. Appl. Phys*. **2004**, *95*, 5691.
(17) Pontes, F. M.; Pinheiro, C. D.; Longo, E.; Leite, E. R.; de Lazaro, S. R.; Varela, J. A.; Pizani, P. S.; Boschi, T. M.; Lanciotti, F. *Mater. Chem. Phys*. **2003**, *78*, 227.
(18) Pontes, F. M.; Pinheiro, C. D.; Longo, E.; Leite, E. R.; de Lazaro, S. R.; Magnani, R.; Pizani, P. S.; Boschi, T. M.; Lanciotti, F. *J. Lumin*. **2003**, *104*, 175.
(19) Longo, E.; Orhan, E.; Pontes, F. M.; Pinheiro, C. D.; Leite, E. R.; Varela, J. A.; Pizani, P. S.; Boschi, T. M.; Lanciotti, F.; Beltran, A.; Andres, J. *Phys. Rev. B* **2004**, *69*.
(20) Pontes, F. M.; Longo, E.; Leite, E. R.; Lee, E. J. H.; Varela, J. A.; Pizani, P. S.; Campos, C. E. M.; Lanciotti, F.; Mastelaro, V.; Pinheiro, C. D. *Mater. Chem. Phys*. **2003**, *77*, 598.

10.1021/cm060386y CCC: $33.50
Published on Web 05/20/2006

interaction of the TiO_5-TiO_6 pair.[21]

Several papers can be found in the literature related to the structural disorder and quantum mechanics calculation.[22,23] These authors used periodic calculations DFT/B3LYP to relate the structural disorder of titanate with the room-temperature PL properties. The applied methodology is based on the atomic displacement to study the charge transfer between TiO_5-TiO_6 clusters and the electronic levels inside the band gap.

Amorphous metal oxides processed by modified Pechini method,[24] called the polymeric precursor method (PPM), displayed intense PL at room temperature. A simple water-based chemical process was used, allowing amorphous metal oxides to be processed at temperatures as low as 300 °C in the form of particles. This method has been used to synthesize nanoparticles of several materials and is based on the chelation of cations by a carboxylic acid, such as citric acid, in an aqueous solution.

According to discussions in the literature there is an order−disorder concept in materials such as glasses,[25] amorphous materials,[26,27] and ceramics[28] to explain some properties of these solid solutions. Such concept is explaining in terms of organization or structural of the material as phase transitions[28] and techniques to determine the order in short, medium, and long ranges.[26,27] In the present work it is proposed to use Raman spectroscopy, XRD, PL emission, and quantum mechanical ab initio calculation to observe and understand the order−disorder at short and long range. In particular, the PL emission result will be used as a tool for observing the increase of the structural order of the compound CT:Sm.

Experimental Section

Materials and Instrumentation. Amorphous and crystalline $Ca_{1-x}Sm_xTiO_3$, $x = 0.05$ (CT:Sm) were synthesized by PPM. To study the order−disorder in the perovskite CT the Sm^{3+} was used as an indicator of the structure order established in the material after certain thermal annealing treatment. Sm^{3+} ion was chosen to replace the Ca^{2+} ion to provoke structural defects in the compound CT:Sm through of the introduction of holes. The Sm^{3+} ion amount was fixed to $x = 0.05$ in the lattice. It was not the interest of this work to observe the influence of the Sm^{3+} amount once the emphasis was the influence of the heat treatment with reference to the increase of the structural order of the solid solution $Ca_{0.95}Sm_{0.05}TiO_3$.

Titanium citrates were formed by the dissolution of titanium(IV) isopropoxide in an aqueous solution of citric acid (60−70 °C). After homogenization of the Ti citrate solution, $CaCO_3$ was slowly added. After complete dissolution of the $CaCO_3$ salt, Sm_2O_3 was first dissolved in nitric acid and gradually added to the Ca−Ti citrate solution. Ethylene glycol was then added to promote polymerization of the mixed citrates by polyesterification reaction between 90 and 120 °C followed by the elimination of water. The molar ratio between citric acid and ethylene glycol was fixed at 60/40 (mass ratio).

The polyester resin was annealed at 300 °C for 2 h. The obtained powder was deagglomerated, and then it was precalcined at 300 °C for 20 h in an oxygen flow to promote oxidation of the organic matter and prepyrolysis without crystallization. After being precalcined, CT:Sm was submitted to a heat treatment at 350, 400, 450, 500, 550, and 600 °C for 2 h in an oxygen flow. CT:Sm powders were structurally characterized by X-ray diffraction (XRD) (Cu Kα radiation) in the mode of $\theta-2\theta$ scan (θ is the diffraction angle), recorded on a Siemens D5000 diffractometer. Such results indicate that the sample is a single phase and could be completely indexed on the basis of an orthorhombic ICDD card no. 42-423 (*Pbnm*). No peaks were observed, neither the ones related to the presence of TiO_2 or Sm_2O_3, nor those indicating the presence of precursors.

Raman data were taken on an RFS/100/S Bruker FT-Raman with a Nd:YAG laser providing an excitation light at 1064.0 nm. The spectral resolution was 4 cm^{-1}, and the 100−700 cm^{-1} spectral range was analyzed. The optical spectrum was obtained in the total reflection mode, using Cary 5G equipment. The PL measurements were realized using a U1000 Jobin-Yvon double monochomator coupled to a cooled GaAs photomultiplier and a conventional photon-counting system. The 488.0 nm exciting wavelength of an argon ion laser was used with the maximum output power of the laser kept within 20 mW. All the measurements were taken at room temperature.

Computer Details. For the theoretical modeling of the CT:Sm samples periodic DFT calculations were used with Becke's three-parameter hybrid nonlocal exchange functional combined with the Lee−Yang−Parr gradient-corrected correlation functional (B3LYP),[19,29] by means of the CRYSTAL98 computational code.[30] Ca, Ti, and O centers have been described in the scheme 86-511d3G, 86411-d(41), and 6-31G*, respectively. In this paper the lattice constants and internal coordinate data were obtained by means of the XRD patterns refinement using the Rietveld method. Sambrano et al.[22] have used this methodology to simulate perovskites of technological interest.

For the auxiliary investigation of the order−disorder of the CT:Sm solid solution the analysis of density of states (DOS) and Mulliken charges was used. However, to associate these results with ordered and disordered material the site Ti atom−TiO_6 was attributed to the ordered structure, whereas for the disordered structure the site Ti atom displacement−TiO_5 was used. This methodology is reported in the literature.[7,21]

Results and Discussion

CT:Sm is a very interesting compound for the study of the PL property due to an order−disorder transition. Ordering or disordering of TiO_5-TiO_6 can be obtained depending on thermal history, with corresponding changes in the PL property. This compound annealed at 350, 400, and 450 °C does not show phonon modes in the Raman spectra and

(21) Orhan, E.; Varela, J. A.; Zenatti, A.; Gurgel, M. F. C.; Pontes, F. M.; Leite, E. R.; Longo, E.; Pizani, P. S.; Beltran, A.; Andres, J. *Phys. Rev. B* **2005**, *71*.
(22) Sambrano, J. R.; Orhan, E.; Gurgel, M. F. C.; Campos, A. B.; Goes, M. S.; Paiva-Santos, C. O.; Varela, J. A.; Longo, E. *Chem. Phys. Lett.* **2005**, *402*, 491.
(23) Orhan, E.; Anicete-Santos, M.; Maurera, M.; Pontes, F. M.; Paiva-Santos, C. O.; Souza, A. G.; Varela, J. A.; Pizani, P. S.; Longo, E. *Chem. Phys.* **2005**, *312*, 1.
(24) Pizani, P. S.; Leite, E. R.; Pontes, F. M.; Paris, E. C.; Rangel, J. H.; Lee, E. J. H.; Longo, E.; Delega, P.; Varela, J. A. *Appl. Phys. Lett.* **2000**, *77*, 824.
(25) Sciortino, F. *Nat. Mater.* **2002**, *1*, 145.
(26) Salmon, P. S. *Nat. Mater.* **2002**, *1*, 87.
(27) Hufnagel, T. C. *Nat. Mater.* **2004**, *3*, 666.
(28) Malibert, C.; Dkhil, B.; Kiat, J. M.; Durand, D.; Berar, J. F.; Spasojevic-de Bire, A. *J. Phys.: Condens. Matter* **1997**, *9*, 7485.
(29) Saunders, V. R. D.; R.; Roetti, C.; Causá, M.; Harrison, N. M.; Orlando, R.; Zicovich-Wilson, C. M.
(30) Dovesi, R.; Saunders, V. R.; Roetti, C.; Causà, M.; Harrison, N. M.; Orlando, R.; Aprà, E. *CRYSTAL98 User's Manual*; Torino, Italy, 1998.

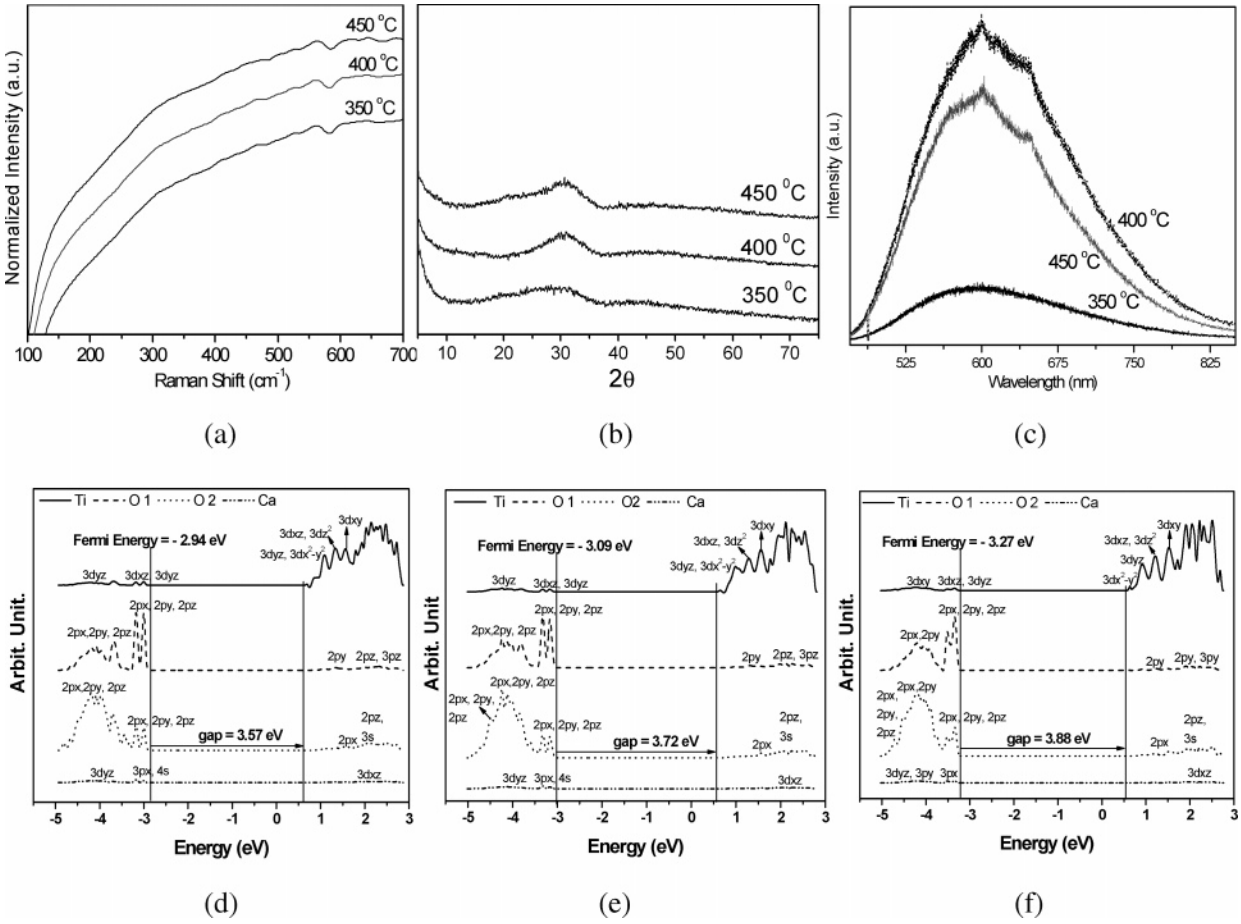

Figure 1. Powder annealed at 350, 400, and 450 °C: (a) Raman spectra, (b) XRD, and (c) broad PL band; projected DOS (d) 0.50 Å displacement, (e) 0.40 Å displacement, and (f) 0.30 Å displacement.

diffraction peaks in the XRD (Figure 1, parts a and b). This confirms that the powders annealed at 350, 400, and 450 °C are disordered in the short and long range. In this temperature range such disorder is characterized by the presence of PL emission intrinsic of the material (Figure 1c). This behavior can be explained as follows. As material begins to become ordered in crystalline form, the intensity of the PL emission drops to virtually zero at room temperature. The TiO_5- and TiO_6-type structures were found in the disordered system, since the PL signal relates to presence of the TiO_5-type structures in a disordered matrix, which was confirmed by XANES.[20] We thus conclude that oxygen deficiency in CT:Sm causes the broad PL band at room temperature. On the other hand, Kan et al.[31] report on blue-light emission at room temperature from Ar^+ irradiated in metallic $SrTiO_3$ showing that the irradiation introduces oxygen deficiencies to a depth of proximally 20 nm from the crystal surface.[31] All luminescence characterization was realized in the same conditions. For samples annealed at 400 and 450 °C the presence of peaks corresponding to the Sm^{3+} ion is noted. DOS results show that displacement Ti atoms, as an approximated form of disorder, cause perturbation in the region near the band gap (Figure 1d−f). There is a decrease of the Fermi energy related to the decrease of the Ti−O bond deformation. The increase of band gap with the decrease of disorder in the Ti−O bond is observed. The O $2p_x$, $2p_y$, and $2p_z$ states are predominant in the valence band (VB), which is located between −5 and −3 eV. Such states are hybridized mainly with Ti $3d_{yz}$, $3d_{xz}$ and Ca $3d_{yz}$, $3p_x$, 4s states. However, not all states are hybridized forming nonbonding states near the gap. These states are responsible for concentrating electrons. The conduction band (CB) is localized between 0.5 and 3 eV, approximately. In this range are mainly localized Ti 3d states with low hybridizations in relation to the O $2p_x$, $2p_y$ states. Note that Ti 3d states are displaced to minor energy levels. These states are responsible for concentrating holes.

Figure 2 shows Raman, XRD, PL, and DOS data for material annealed at 500 and 550 °C. This is the main point of the order−disorder transition because in this temperature range occurs the increase of the order in this system. Raman spectra of the powder annealed at 500 and 550 °C present Raman phonon modes (Figure 2a), indicating a short-range order. Particularity, the spectrum to 550 °C (Figure 2a) does not show high resolution (still cannot complete order), but there is evidence of some O−Ti−O bending modes between 150 and 350 cm^{-1} (Table 1).

However, a long-range order is not yet observed since that the material annealed at 500 °C does not present diffractions peaks in the XRD spectrum (Figure 2b). At this condition the presence of visible PL emission related to samarium is expected (Figure 2c). Hence, the decrease of broad PL band intensity between 450 and 550 °C is associated with the decrease or even the extinction of the TiO_5-type structures.

(31) Kan, D. S.; Terashima, T.; Kanda, R.; Masuno, A.; Tanaka, K.; Chu, S. C.; Kan, H.; Ishizumi, A.; Kanemitsu, Y.; Shimakawa, Y.; Takano, M. *Nat. Mater.* **2005**, *4*, 816.

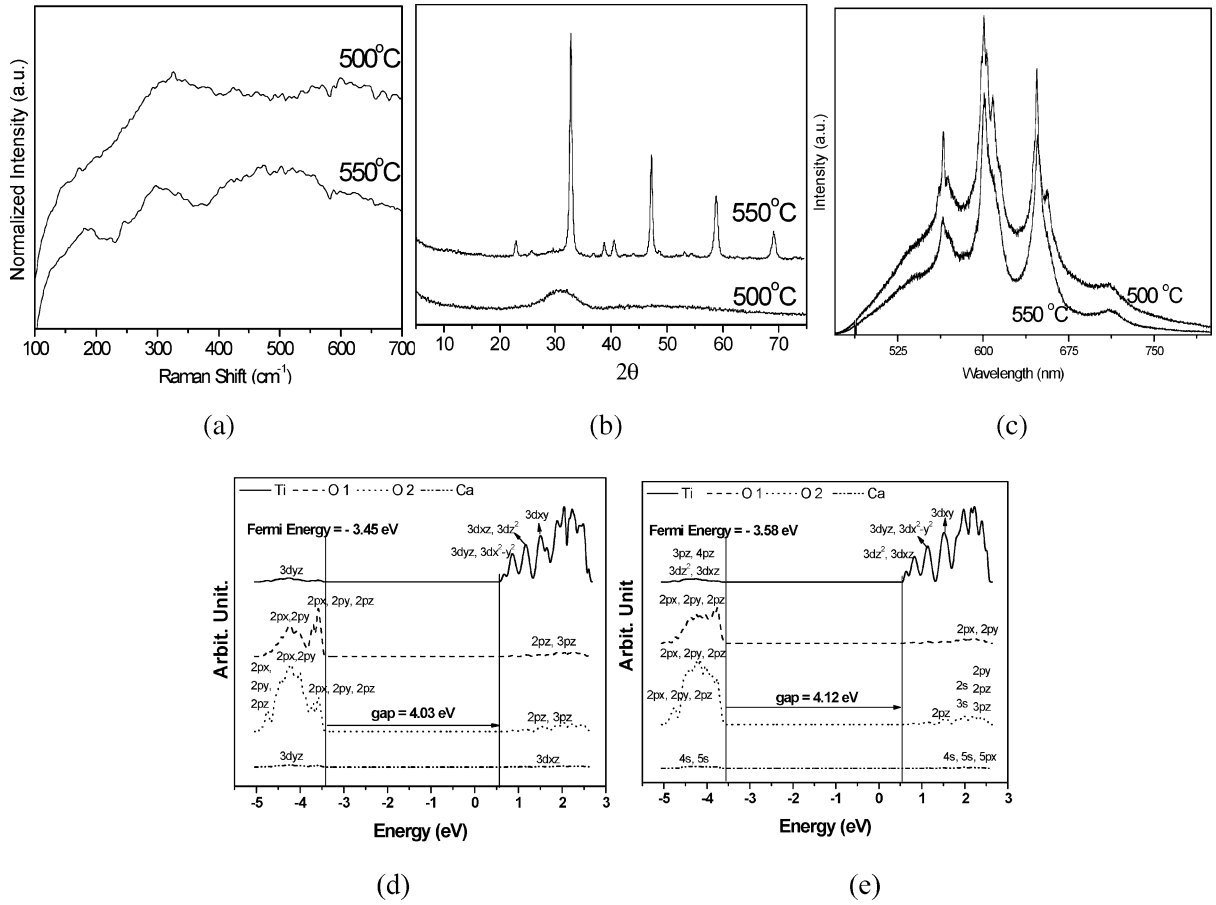

Figure 2. Powder annealed at 500 and 550 °C: (a) Raman spectra, (b) XRD, (c) broad PL band; DOS (d) 0.20 Å displacement and (e) 0.10 Å displacement.

Table 1. Frequencies (cm^{-1}) of Unpolarized Raman Bands and Their Assignments for CT:Sm

	label corresponding to Figure 3a	ref 27	ref 28	ref 29	this work
Ca−TiO_3 lattice mode	a				128
	b	155	153		160
O−Ti−O bending modes	c	180	178	183	181
	d	226	222	225	220
	e	247	244	247	245
	f	286	281	288	295
	g	337	333	339	339
Ti−O_3 torsional modes	h	471	467	470	471
	i	495	490	494	495
Ti−O symmetric stretching	j	639		641	644

As a result there is a reduction in the number of structural short- and long-range defects which can generate localized states in the band gap as well as inhomogeneous charge distribution in the cell.

Powder annealed at 550 °C presents a short-range order as observed by phonon modes in the Raman spectra (Figure 2a). In this spectrum O−Ti−O bending and Ti−O_3 torsional modes can be observed (Table 1). In this condition there are diffractions peaks in the XRD spectrum establishing a long-range order−periodicity (Figure 2b). Despite that the material presents short- and long-range order, it still displays a broad PL band, indicating that it is not completely ordered (Figure 2c). Considering these results, it can be proposed that, in this condition, the material does not present a complete order.

It can be observed in Figure 2c that the material is not totally organized at long range, but the effect of the crystalline field is to establish an order surrounding the samarium ion producing a peak definition referred to as the intrashell f of the Sm^{3+} ion.

Figure 2, parts d and e, shows DOS results due to displacement of 0.20 and 0.10 Å in the Ti−O bond. It can be observed that in the VB the O $2p_x$, $2p_y$, $2p_z$ states are located from the −4.6 to −0.6 eV range. It is also noted that there is a change in the hybridization between the O 2p and Ti 3d states. The Ti $3d_{yz}$ state changes to Ti $3d_{z^2}$, $3d_{xz}$ states; this is correlated to stabilization of the Ti−O bond in the *z*-direction, alternating the charge-transfer direction in relation to these states. In the CB an inversion of position occurs between the Ti $3d_{yz}$, $3d_{x^2-y^2}$ and Ti $3d_{xz}$, $3d_{z^2}$ states; this indicates that the stabilization of the Ti $3d_{z^2}$ state is the major one responsible by the Ti−O bond in the *z*-direction. According to this decrease in the deformation of the Ti−O bond the Ca states can be stabilized demonstrating that

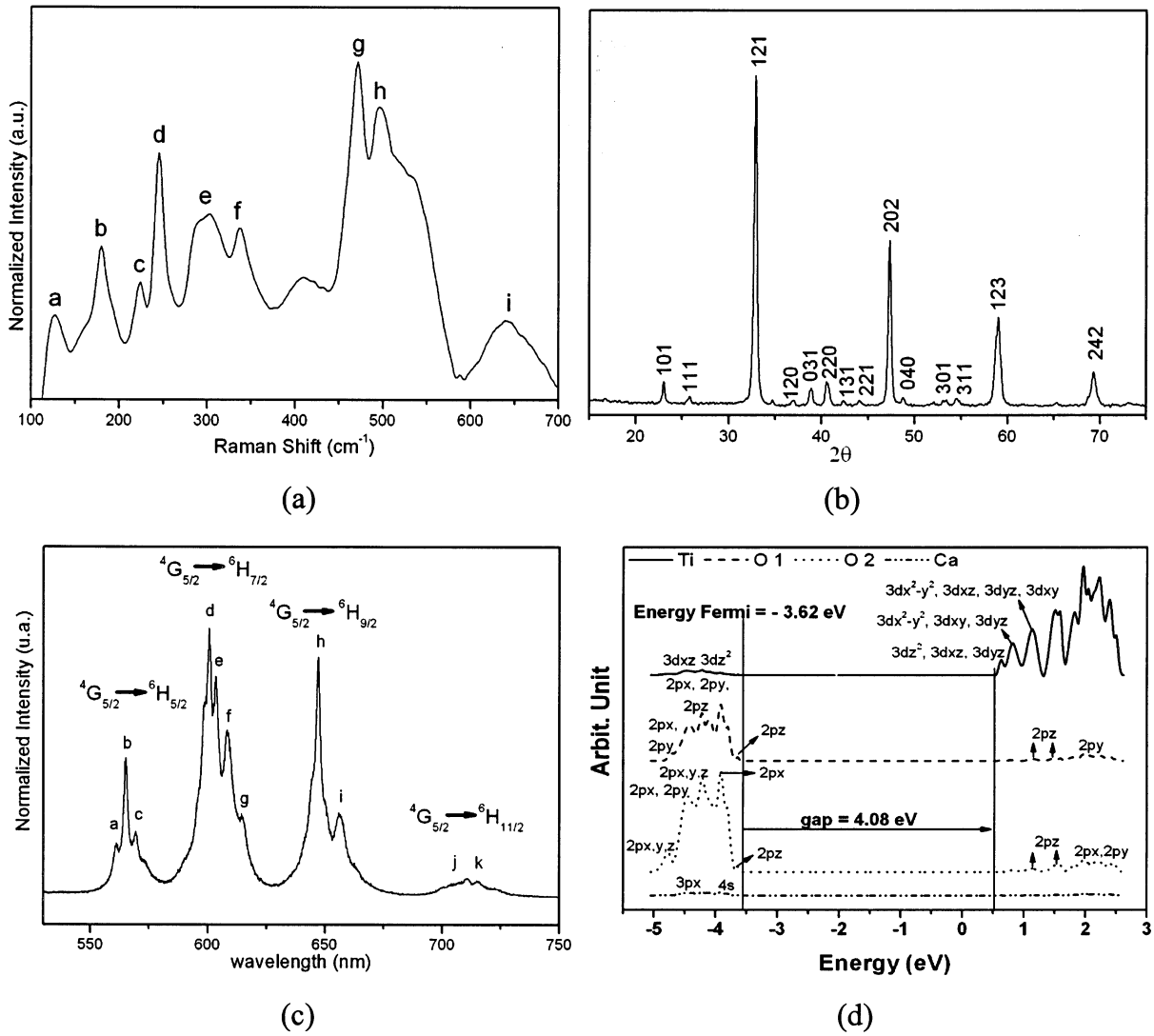

Figure 3. Powder annealed at 600 °C: (a) Raman spectra, (b) XRD, (c) emission spectra of Sm, (d) projected DOS crystalline.

despite the small contribution in this energy range those states are influenced.

Complete order is reached for the sample annealed at 600 °C. This behavior is observed by the presence of all phonon modes in the Raman spectra (Figure 3a) that is consistent and indicates the orthorhombic phase of ordered CT:Sm.[32−34] Peaks at 128 and 160 cm^{-1} are observed and attributed to $Ca-TiO_3$ lattice modes (Table 1), demonstrating an ordered system when compared with that of Figure 2a. Such attribution was based in Parlinski et al.'s[35] work. Figure 3b demonstrates the definition of the diffraction peaks that are comparable to the result of the XRD for $CaTiO_3$.[36,37] This is related to establishment of the long-range order or periodicity. In terms of PL (Figure 3c), the observed result demonstrates that only samarium emission is evident due to part of the charge-transfer band (CTB) of the $Sm^{3+}-O^{2-}$ bond, and the latter is from the f−f transitions within the Sm^{3+} $4f^5$ electron configuration (Table 2).[38−40] Hence, this powder annealed at 600 °C presents short- and long-range order. So this material presents phonon modes in the Raman spectra (Figure 3a) indicating a short-range ordering. XRD peaks (Figure 3b) confirm the long-range ordering (periodicity). The absence of the broad PL band corroborates with the complete order of this material (Figure 3c).

It is interesting that, at room temperature, the XRD results show a long-range order or periodicity for CT:Sm annealing at 550 °C, while the Raman modes are defined up to 600 °C. This difference was understood by the fact that X-ray probes the overall long-range order, whereas Raman scattering probes the short-range structural order.

However, it has long been known that structural organizations intermediate between discrete chemical bonds (short-

(32) Balachandran, U.; Eror, N. G. *Solid State Commun.* **1982**, *44*, 815.
(33) Qin, S.; Wu, X.; Seifert, F.; Becerro, A. I. *J. Chem. Soc., Dalton Trans.* **2002**, 3751.
(34) Zheng, H.; de Gyorgyfalva, G.; Quimby, R.; Bagshaw, H.; Ubic, R.; Reaney, I. M.; Yarwood, J. *J. Eur. Ceram. Soc.* **2003**, *23*, 2653.
(35) Parlinski, K.; Kawazoe, Y.; Waseda, Y. *J. Chem. Phys.* **2001**, *114*, 2395.
(36) Vashook, V.; Vasylechko, L.; Knapp, M.; Ullmann, H.; Guth, U. *J. Alloys Compd.* **2003**, *354*, 13.
(37) Qin, S.; Becerro, A. I.; Seifert, F.; Gottsmann, J.; Jiang, J. Z. *J. Mater. Chem.* **2000**, *10*, 1609.
(38) Makishim, S.; Yamamoto, H.; Tomotsu, T.; Shionoya, S. *J. Phys. Soc. Jpn.* **1965**, *20*, 2147.
(39) Kodaira, C. A.; Brito, H. F.; Teotonio, E. E. S.; Claudia, M.; Felinto, M.; Malta, O. L.; Brito, G. E. S. *J. Braz. Chem. Soc.* **2004**, *15*, 890.
(40) Honma, T.; Benino, Y.; Fujiwara, T.; Sato, R.; Komatsu, T. *J. Phys. Chem. Solids* **2004**, *65*, 1705.

Table 2. Energy Levels and Wavelength (nm) for the Intraconfigurational Transitions of the Sm^{3+} in CT:Sm

transition	label corresponding to Figure 3c	ref 34	ref 35	this work
$^4G_{5/2} \rightarrow {}^6H_{5/2}$	a	563	565	561
	b	564		565
	c	568		569
$^4G_{5/2} \rightarrow {}^6H_{7/2}$	d	597	600	600
	e	600		603
	f	603		608
	g	605		614
$^4G_{5/2} \rightarrow {}^6H_{9/2}$	h	649	645	647
	i	652		656
$^4G_{5/2} \rightarrow {}^6H_{11/2}$	j	704	705	710
	k	715		714

range structural order) and periodic crystalline lattices (long-range structural order) are present in CT:Sm. These features correspond to large real-space distances in the materials, and understanding their origin is key to unraveling details of intermediate-range order. Here, we employ principles of the Sm emission spectrum to design specific patterns of intermediate-range order within amorphous CT:Sm networks (Figures 2c and 3c).

PL comportment for the CT:Sm compound can be summarize as follows: the intensity of the PL emission, previously discussed, passes alterations according with the evolution of the structural order of the CT:Sm material. It is observed that this alteration passes a maximum of emission at 400 °C and, later, there occurs a decrease of the intensity of emission followed by the phenomenon vanishing at 600 °C. The PL remainder is due to the Sm^{3+} ion. It is proposed that PL emission is analysis as a possible tool of structural analysis, mainly between disordered and ordered phases.

DOS calculations for the crystalline CST are shown in Figure 3d. A great degeneracy among Ti 3d states is observed mainly in the 0.6−1.3 eV range. Hybridization between Ti 3d states and O 2p states in the range from −4.6 to 4.0 eV is also observed. The O 2p states also acquire degeneracy in the VB. Ca states are stabilized in the direction to the VB.

It can be noted in the projected DOS that the contributions near the Fermi energy are nonbonding states. These states are contracted (degeneracy) leading to the decrease of system distortion. Such behavior is related to Jahn−Teller symmetry, i.e., molecular distortion is associated with perturbations in the electronic degeneracy[41,42] of the atoms. Considering that the degeneracy of these states contributes to widening of the band gap and of the Fermi energy stabilization, the disorder in solids cause both the degeneracy and destabilization in the localized states of the atoms, supporting the PL phenomena in amorphous solids.

By previous description increasing the annealing temperature causes an increase in the structural order, which is responsible for changing the PL intensity. The PL intensity increased gradually for the powders annealed at 350 and 400 °C, and for the powders annealed at 450, 500, 550, and 600 °C the PL intensity decreased gradually. PL is associated to the presence of TiO_5 and TiO_6 clusters[19,21] responsible by introduction of delocalized electronic levels nearest the VB. Such delocalized levels yield energy levels inside the band gap, and these act as electron−hole pairs.

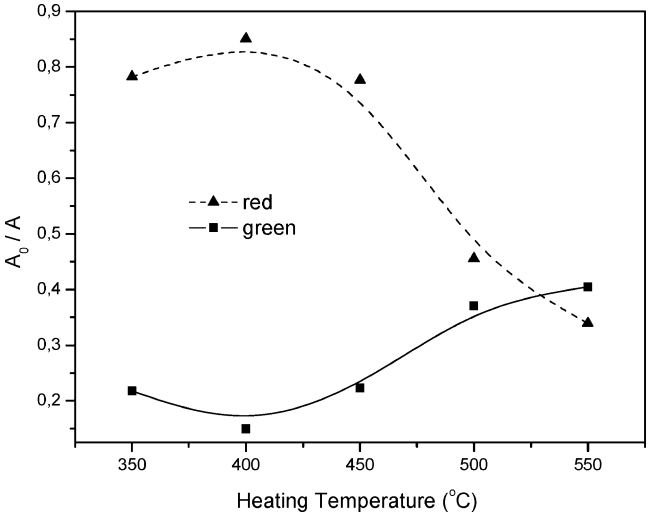

Figure 4. Relative contribution of high-energy (green) and low-energy (red) PL emission as function of annealing temperature.

PL observed for the CT:Sm shows that the transitions in this material are of the intermediate energy levels between the VB and the CB, since that the excitation energy is smaller than the gap energy of this material. To investigate this behavior the PL curves (Figures 1c and 2c) were decomposed into two curves. It was observed that one curve is centered in the smaller wavelength region, the green region, and the other curve is located in the larger wavelength region, the red region. These behaviors represent transition levels inside the band gap.

By increasing the calcining temperature in this solid solution, the transition of amorphous−crystalline states is provoked in consequence of the increase in the amount of TiO_6 clusters, increasing the order in the solid. It is important to observe that there is a contraction of the VB due to the increase of order of the system (TiO_6), resulting in the increase of band gap energy. Such results are evidence that the order−disorder (TiO_5−TiO_6) present in the material is the major factor responsible for the degeneracy among electronic states yielding delocalized levels fundamental to PL phenomena.

DOS calculations for the crystalline CST are shown in Figure 3d. A great degeneracy among Ti 3d states is observed mainly in the 0.6−1.3 eV range. Hybridization between Ti 3d states and O 2p states in the range from −4.6 to 4.0 eV is also observed. The O 2p states also acquire degeneracy in the VB. Ca states are stabilized in the direction to the VB.

Figures 1c, 2c, and 3c show the broad PL band spectra of CT:Sm powders annealed at 350−600 °C for 2 h. These broad band spectra can be deconvoluted into two Gaussian-type functions, one peaking red band and the other one a green band. Figure 4 was obtained by dividing the area of each decomposed broad PL band curve (A_0) by total broad

(41) Lucovsky, G.; Fulton, C. C.; Zhang, Y.; Zou, Y.; Luning, J.; Edge, L. F.; Whitten, J. L.; Nemanich, R. J.; Ade, H.; Schlom, D. G.; Afanase'v, V. V.; Stesmans, A.; Zollner, S.; Triyoso, D.; Rogers, B. R. *IEEE Trans. Device Mater. Reliab.* **2005**, *5*, 65.
(42) O'Brien, M. C. M.; Chancey, C. C. *Am. J. Phys.* **1993**, *61*, 688.

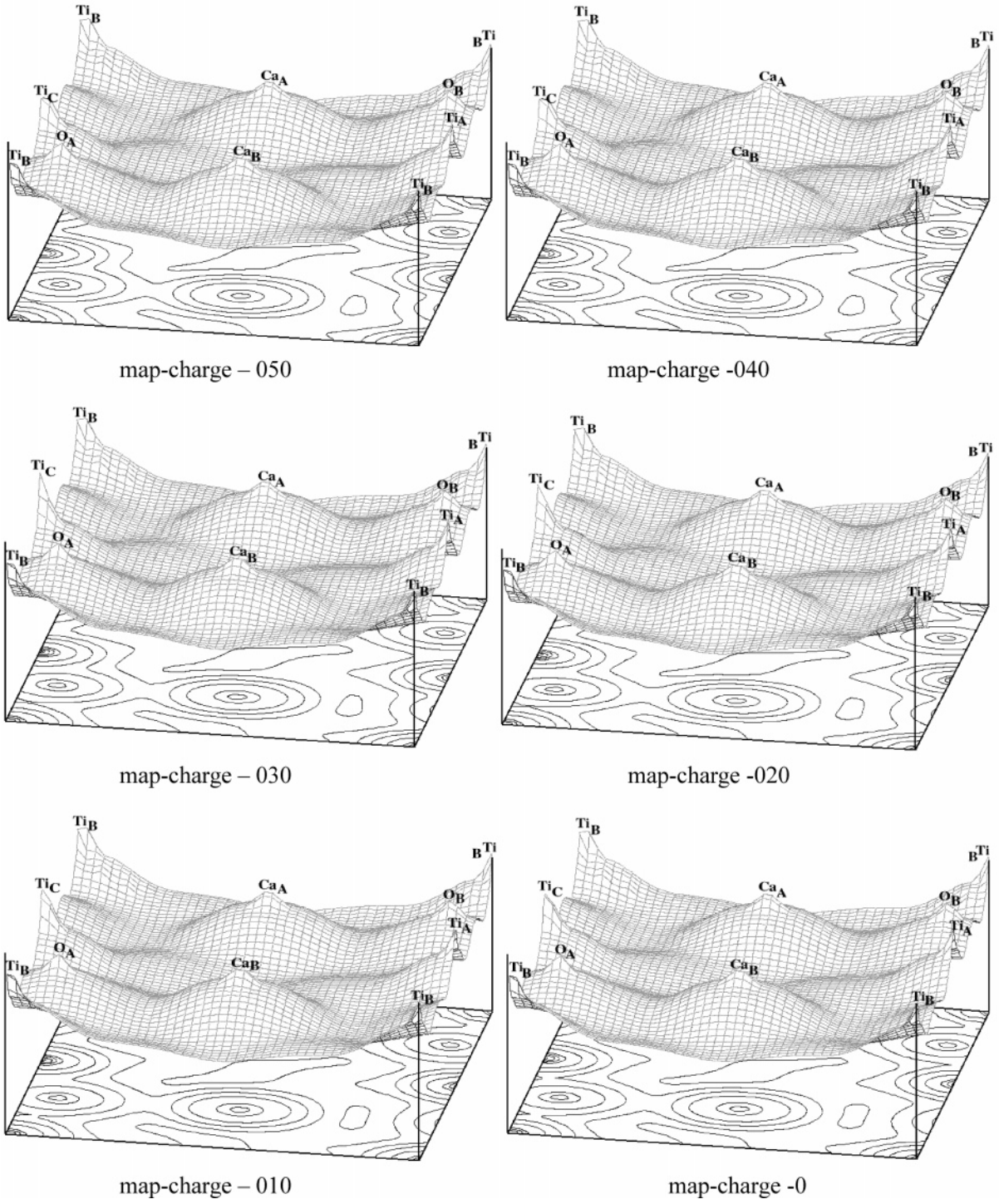

Figure 5. Charge density contour and surface plots (100) for several Ti−O displacements.

PL band area (*A*). In these plots (Figure 4), it is observed that the green and red components reach a minimum and maximum at 400 °C, respectively. For the green curve, intermediate transition levels are lower than that observed in the red curve. Consequently, those levels have a point in common, located in the interception of the curves. Afterward the intermediate levels of larger energy (green) overcome the intermediate levels of smaller energy (red). The interception of these curves occurs at approximately 529 °C. Hence, the region before the interception shows a larger disorder than order and after that point a larger order than disorder. This is in accordance with our previous investigations on titanates where the higher the heat-treatment temperature (550 °C), the rarer pentacoordination of titanium and the weaker the broad PL band emission (Figure 2c). Following the example of Macke,[43] it is possible to relate the green and red components of the broad PL bands to one particular type of titanium coordination coexisting in the structure as observed by Ponader et al.[44] who detected the presence of hexa- and pentacoordinated titanium in titano−silicate glasses. The red component must somehow be limped with

(43) Macke, A. J. H. *J. Solid State Chem.* **1976**, *18*, 337.
(44) Ponader, C. W.; Boek, H.; Dickinson, J. E. *J. Non-Cryst. Solids* **1996**, *201*, 81.

Table 3. Mulliken Charges Distribution (*Q*) to TiO_5−TiO_6 Clusters in the (100) Plane

X	Ti_BO_6	Ti_AO_5	Ti_CO_5
0.5 0	−2.62	−1.32	−1.47
0.4 0	−2.62	−1.35	−1.45
0.3 0	−2.63	−1.40	−1.40
0.2 0	−2.63	−1.40	−1.40
0.1 0	−2.63	−1.40	−1.40
0.0 0	−2.64		

the pentacoordinated titanium and the green component somehow with the hexacoordinated titanium. The crystalline, fully ordered phase (600 °C) does not present any broad PL band at all when excited with the 480 nm line of the argon ion laser, only the samarium.

In previous papers,[9,19,21] the results of PL for amorphous materials at room temperature were attributed to the charge-transfer effect among TiO_5−TiO_6 clusters. So it is important to analyze the charge transfer for this system. Analyses of Mulliken charge transfer have been regularly used in the literature to elucidate this phenomenon.[21,45] The choice of a Mulliken partition is arbitrary, since there is no unique method of performing the partition of the charge density. In this paper the charge density will be used to evaluate the distribution of charge among the system models. The main factor in these models is the choice of Ti atom displacement direction. This direction was chosen after analysis of the charge map distribution (Figure 5). In this charge map distribution is observed the behavior of the charge density for formation of the TiO_6 clusters with the decrease of the displacement of the Ti_A and Ti_C atoms. This formation is characterized by the covalent nature between Ti_A−O_B and Ti_C−O_A bonds. Nevertheless, note that there are different atom denominations due to the different Mulliken charges assumed according to the chosen displacement.

Results of Mulliken charge to TiO_5−TiO_6 clusters are shown in Table 3. In this table a decrease of charge transfer between the TiO_5−TiO_6 clusters is observed due to the increase of the system symmetry. However, in this orthorhombic system different displacements of Ti_A and Ti_C lead to different amounts of TiO_5 clusters. Such charge transfer between TiO_5−TiO_6 clusters is similar to PL results (Figures 1c, 2c, 3c) that shown a decrease of charge-transfer associated to the annealing temperature of the CT:Sm powder. Hence, the displacement proposed yields a charge transfer from the center to the surrounding. This is similar to the concept of order−disorder,[28] i.e., an effect in a localized point of the structure affects neighboring points of this structure.

(45) Orhan, E.; Pontes, F. M.; Santos, M. A.; Leite, E. R.; Beltran, A.; Andres, J.; Boschi, T. M.; Pizani, P. S.; Varela, J. A.; Taft, C. A.; Longo, E. *J. Phys. Chem. B* **2004**, *108*, 9221.

Conclusions

In conclusion, system ordering at short, intermediate, and long range was accompanied for the $Ca_{0.95}Sm_{0.05}TiO_3$ using Raman, broad PL band, Sm spectrum emission, and XRD characterization. Raman data related to short-range order shows that the material is organized at 500 °C. XRD results demonstrated that the long-range order is established at 550 °C. This determines that short-range order is organized first in relation to long-range order. However, the phenomenon of PL at room temperature is not observed in the crystalline structure at 600 °C. The introduction of Sm^{3+} ion in the bulk CT proportioned to observe that the PL emission of the disordered CT:Sm compound is independent of the PL emission of the Sm^{3+} ion. Analyses based in broad PL and Sm spectrum emission phenomenon have shown that it is possible to accompany this behavior in short and long range to CT:Sm in association to the order−disorder concept. These results are related to intermediate energy levels inside the band gap as demonstrated by the peak area analysis and quantum mechanical modeling. Disorder in solids provokes degeneracy and destabilization in the localized states of the atoms acting as electron−hole pairs and supporting the broad PL band phenomena. Electronic levels are fundamental to understanding the order−disorder process in the solid state.

Acknowledgment. The authors gratefully acknowledge the financial support of the Brazilian research financing institutions FAPESP/CEPID, CNPq, and CAPES. Computer facilities of the Molecular Simulation Laboratory (UNESP-BAURU) are also acknowledged.

CM060386Y